

1 **Supplementary Information**

2

3 **Functional and metabolic alterations of gut microbiota in children with**  
4 **new-onset type 1 diabetes**

5

6 **Yuan et al**

7

8

9

10

11

12

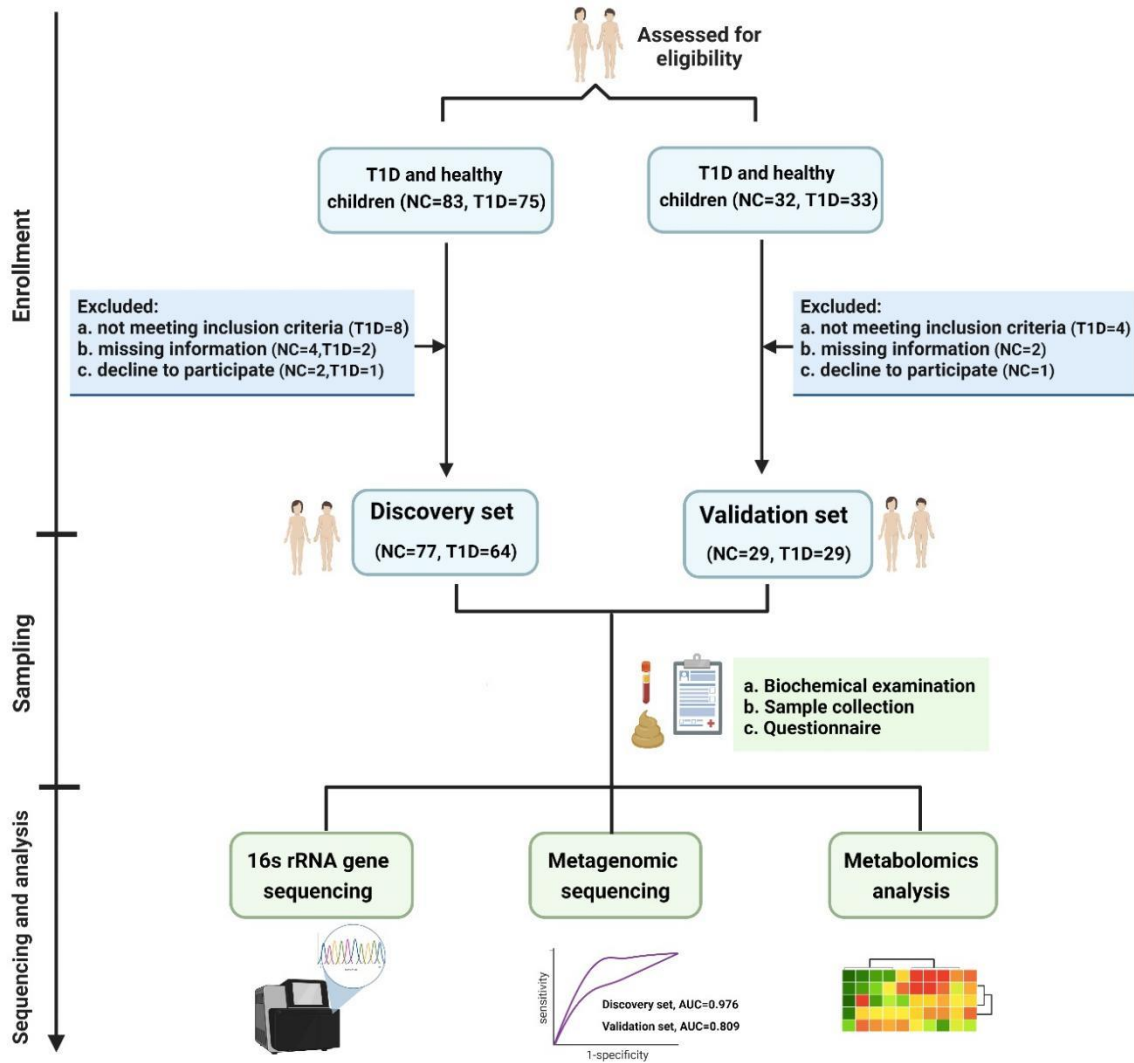
13

14

15

16

17



18 **Supplementary Figure 1. Flow chart illustrating the procedures of the study.** Created with BioRender.com

19

20

21

22

23

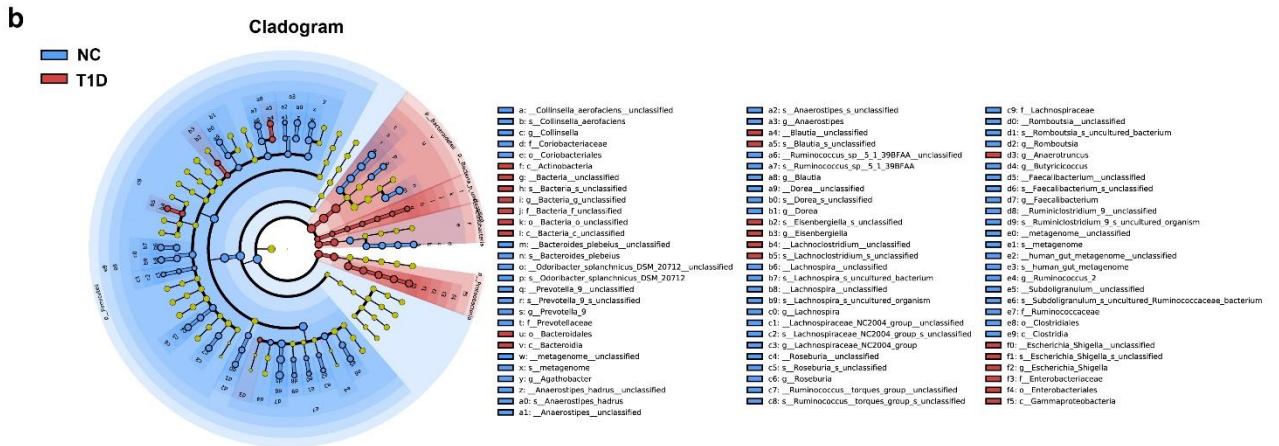
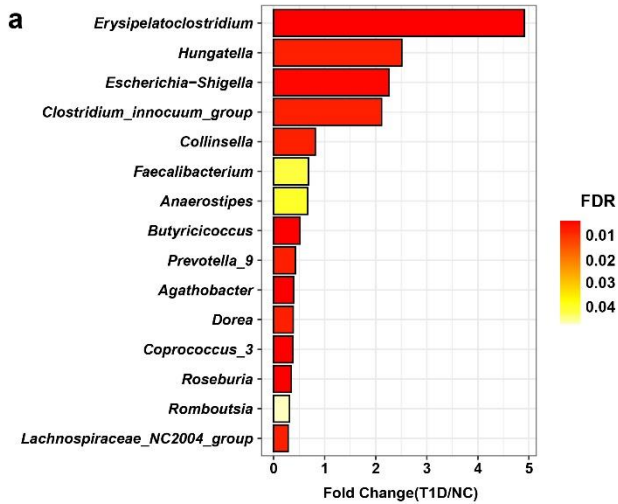
24

25



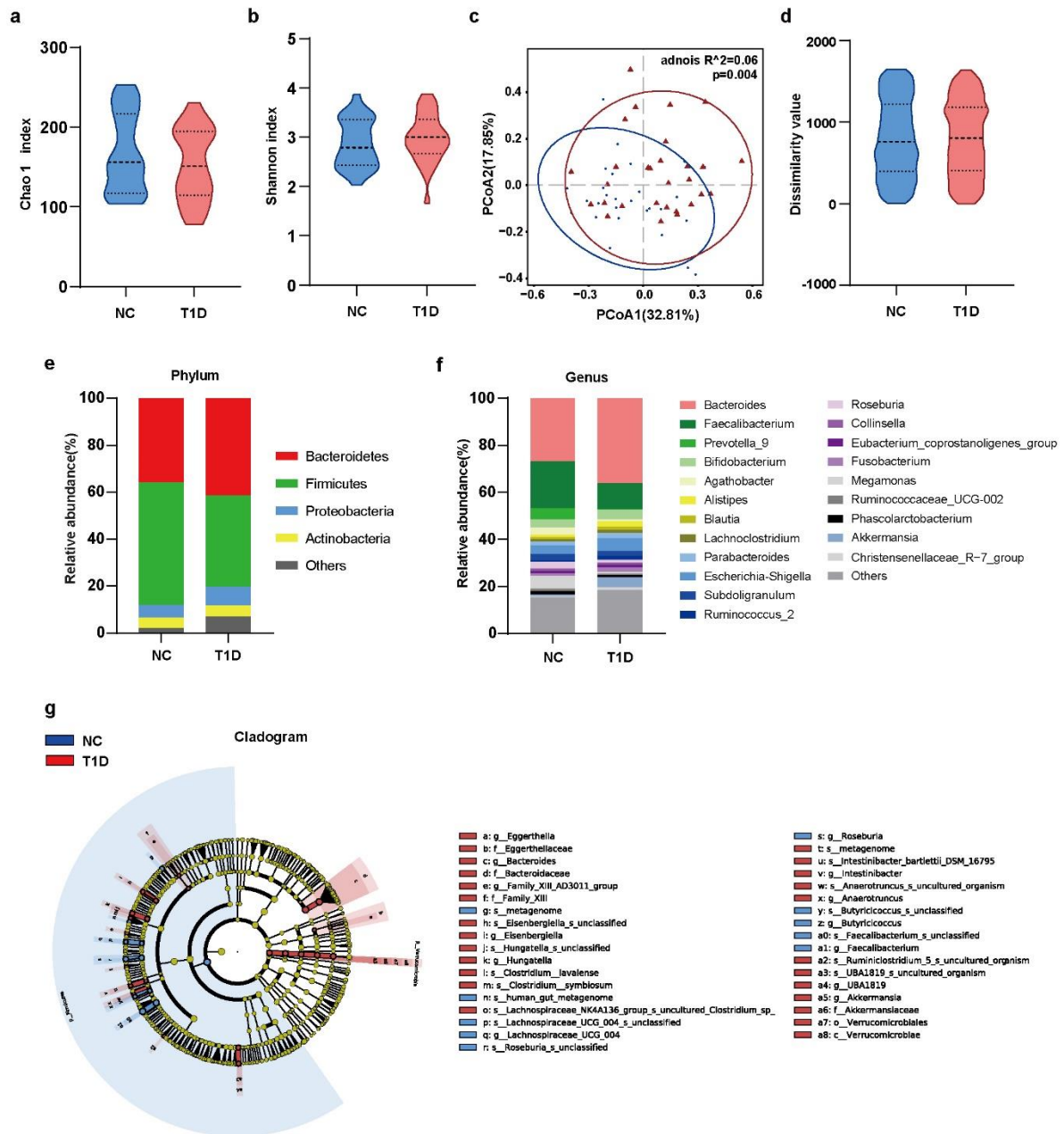
26 **Supplementary Figure 2. Map of sampling area in this study.** The red icons represent the nine sampling  
 27 regions including Harbin, Changchun, Taiyuan, Jinan, Zhengzhou, Suzhou, Shanghai, Nanchang, and Fuzhou  
 28 in China. The Chinese map was generated by the public standard map online service (GS (2019)1676)  
 29 (<http://bzdt.ch.mnr.gov.cn/>).

30  
 31  
 32  
 33  
 34  
 35  
 36  
 37  
 38  
 39

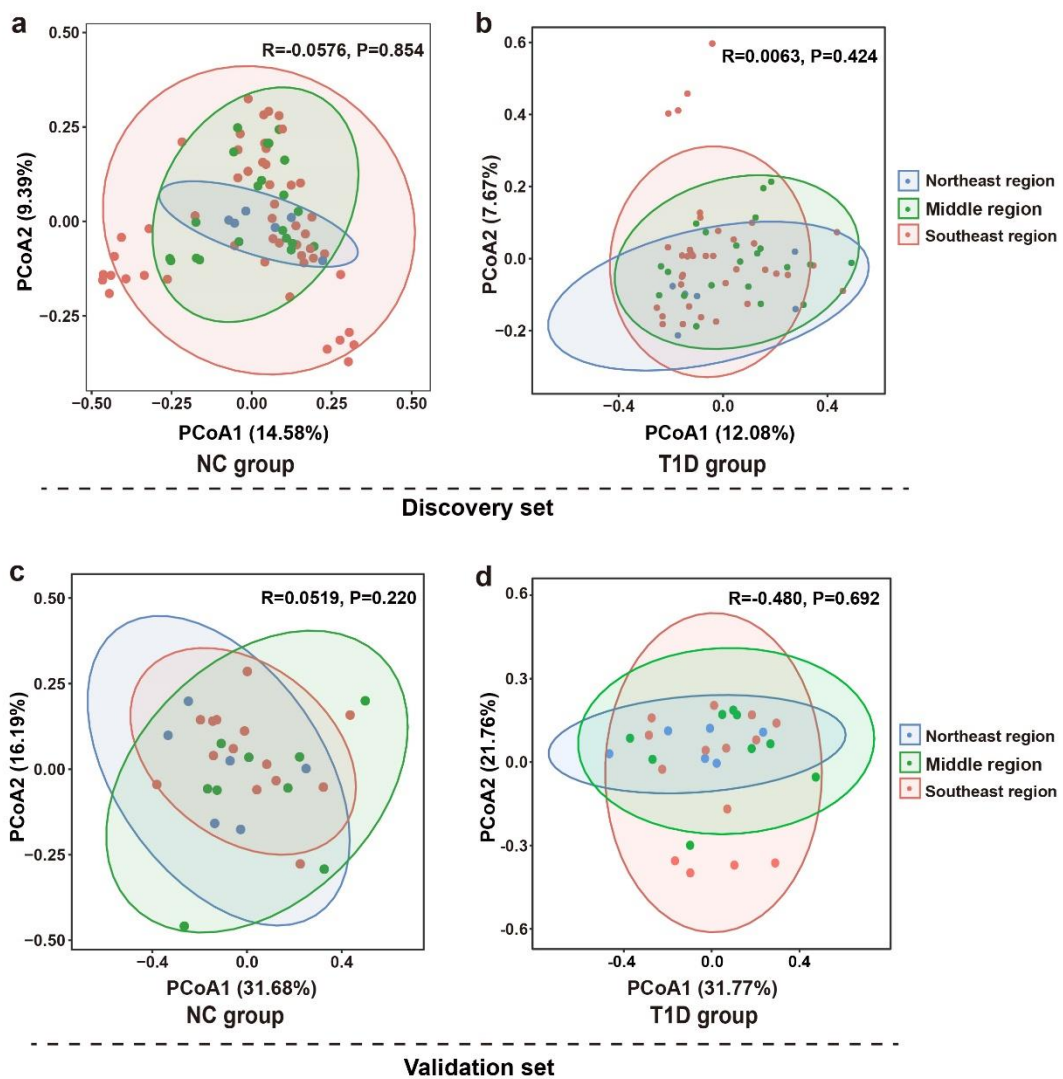


40 **Supplementary Figure 3. Microbial communities in the discovery set.** (a) Foldchange of 15 genera with the  
 41 most significant differences based on the Wilcoxon rank-sum test. (b) LEfSe taxonomic cladogram of differential  
 42 genera between the NC and T1D group. NC: n= 77, T1D: n = 64.

43  
 44  
 45  
 46  
 47  
 48  
 49  
 50  
 51

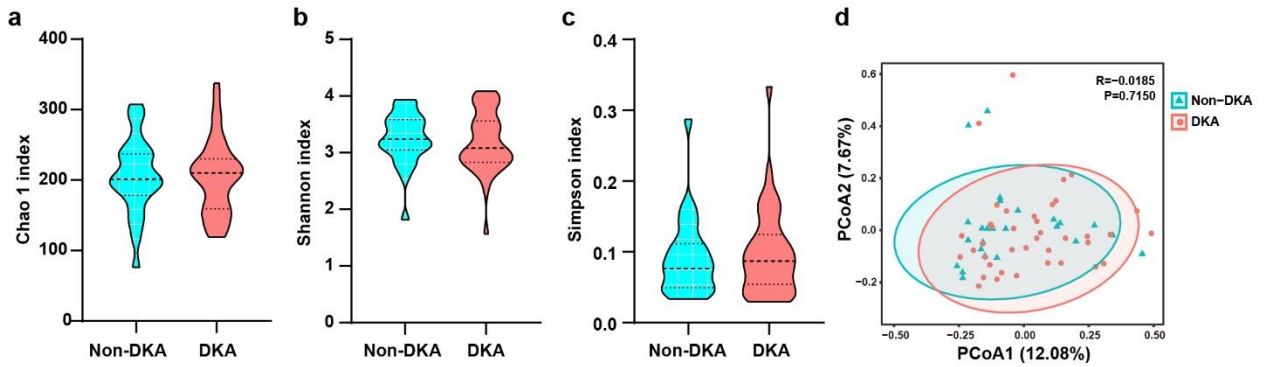


52 **Supplementary Figure 4. The shift of gut microbiota based on 16S rRNA gene sequencing in the**  
 53 **validation set.** (a, b) The microbial community richness (Chao 1 index; a) and diversity (Shannon index; b).  
 54 (c,d) PCoA analysis based on weighted Unifrac distance (c) and analysis of similarities (ANOSIM) (d). (e, f)  
 55 Comparisons of relative abundance of microbial taxa at the phylum (e) and genus (f) level. (g) Cladogram  
 56 generated by LefSe analysis indicating differences in bacterial taxa between the NC and T1D group. The color  
 57 of discriminative taxa represents the taxa more abundant in the corresponding group (NC in blue, T1D in red).  
 58 NC: n= 29, T1D: n = 29. Violin plots show the median, quartiles, and min/max values. Two-sided Wilcoxon rank-  
 59 sum test.



60 **Supplementary Figure 5. PCoA of microbial communities based on the 16S rRNA gene sequencing**  
 61 **profiles at different regions in the discovery set (a,b) and validation set (c,d), respectively.** The northeast  
 62 region includes Harbin and Changchun. The middle region includes Taiyuan, Jinan, and Zhengzhou. The  
 63 southeast region includes Suzhou, Shanghai, Nanchang, and Fuzhou.

64  
 65  
 66  
 67  
 68  
 69



Discovery set

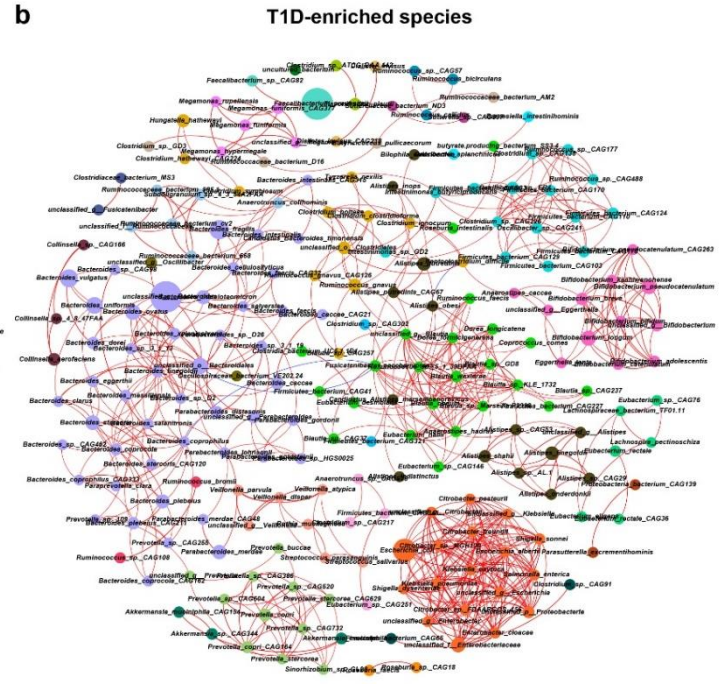
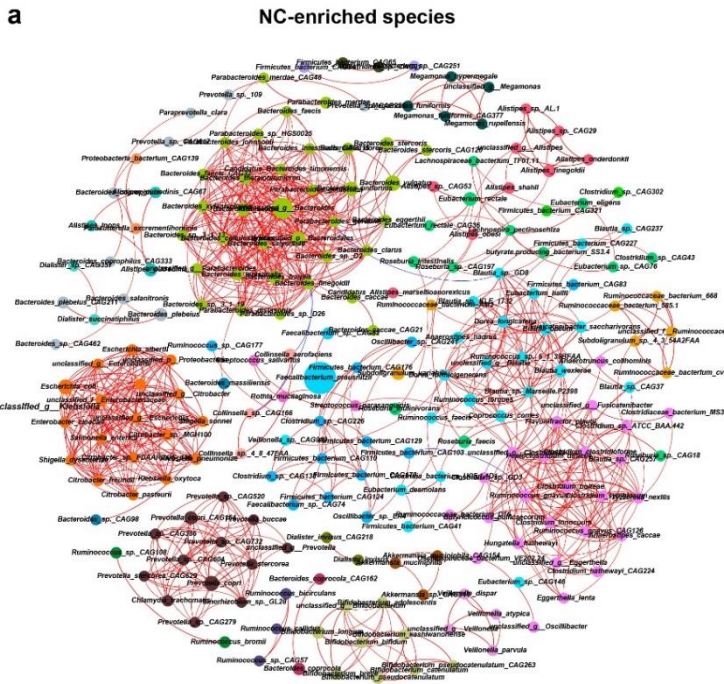
Validation set

70 **Supplementary Figure 6. Microbial communities based on the 16S rRNA gene sequencing profiles in**  
 71 **the DKA and Non-DKA group.**  $\alpha$  diversity (Chao 1, Shannon and Simpson index) in the discovery set (a-c)  
 72 and validation set (e-g), respectively. PCoA plot in the discovery set (d) and validation set (h), respectively.  
 73 Violin plots show the median, quartiles, and min/max values. Two-sided Wilcoxon rank-sum test.

74

75

76

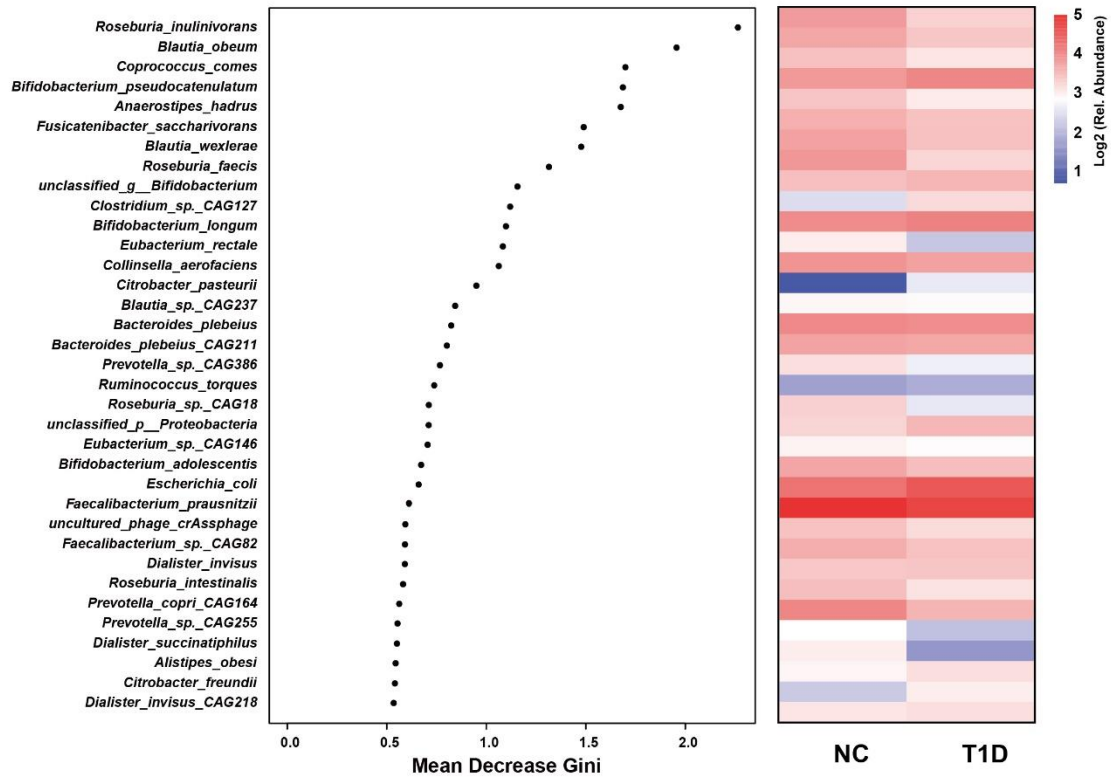


77 **Supplementary Figure 7. The gut microbiota divergence in NC and T1D group based on the**  
 78 **metagenomic sequencing data in the discovery set. (a, b) Co-occurrence network in the NC and T1D group**  
 79 **based on the Spearman correlation algorithms. The node size indicates the relative abundance of each bacteria**  
 80 **per group. Correlations were identified by the absolute value of Sparcc's coefficient > 0.60 and  $p < 0.05$ .**

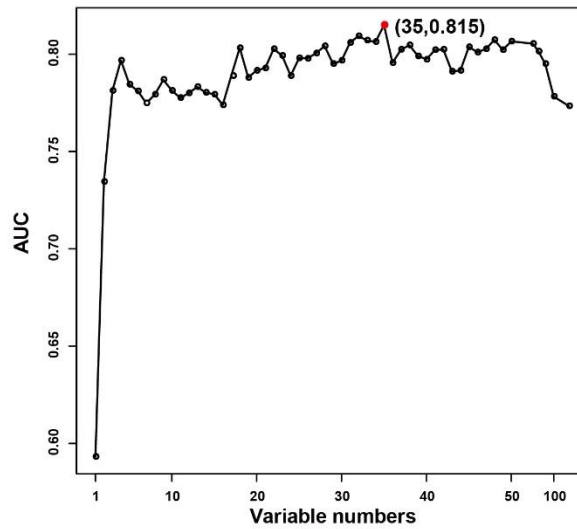
81  
82  
83  
84  
85  
86  
87  
88  
89  
90



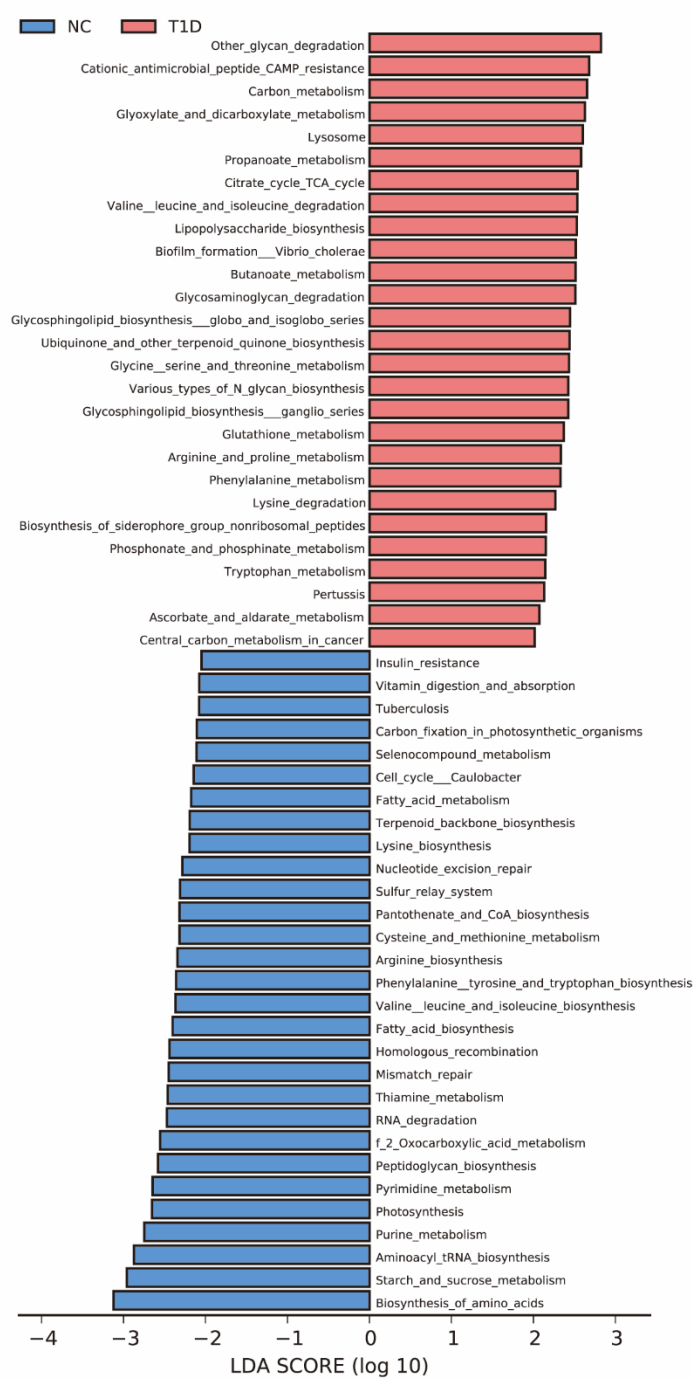
a



b

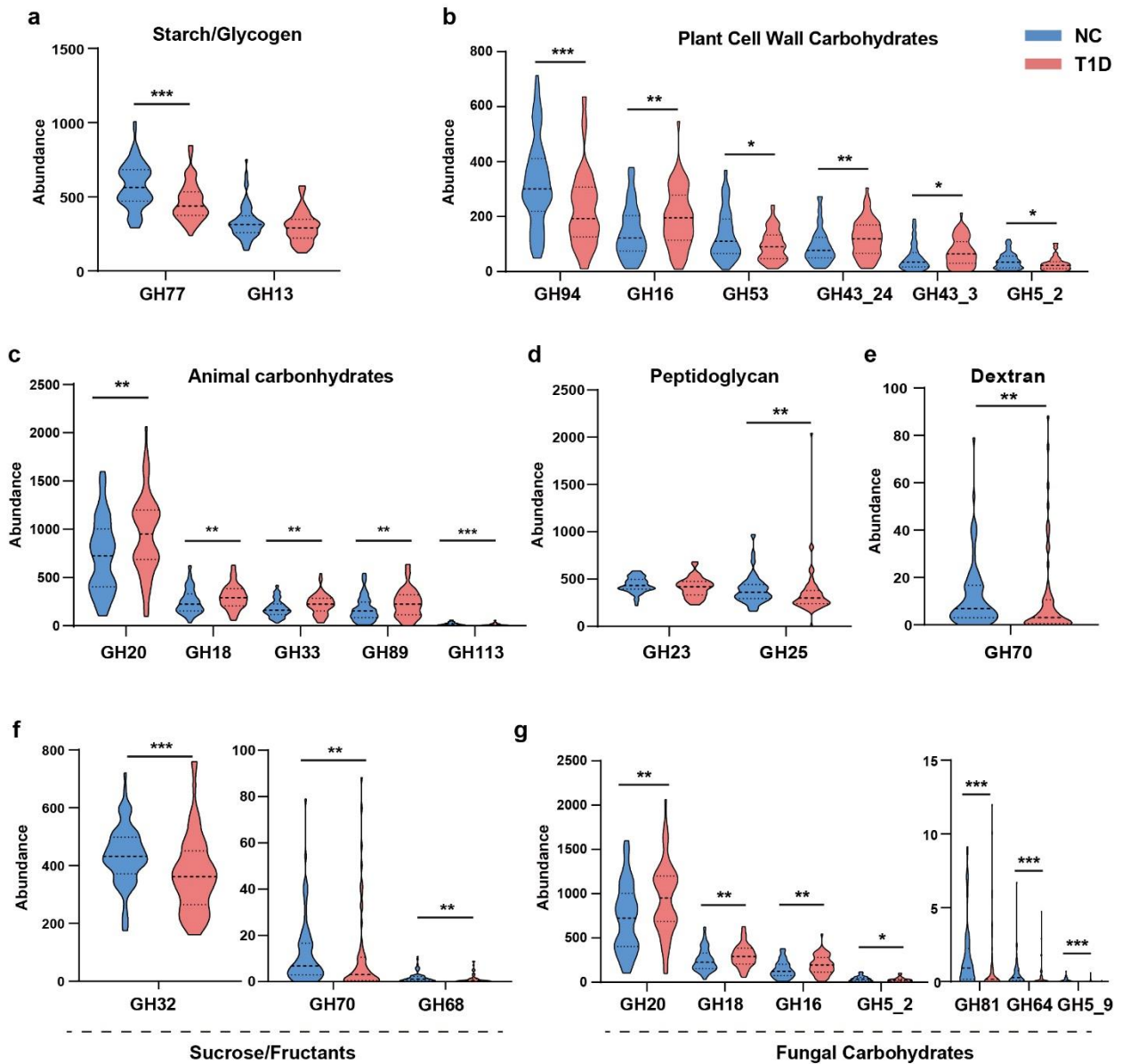


91 **Supplementary Figure 8. Discriminatory species identified by Random Forest analysis.** (a) The top 35  
92 most important species identified by Random Forest analysis (metagenomically derived species with a relative  
93 abundance of more than 2.5% at least in one sample). (b) The area under the curve based on the cross-  
94 validation of the random forest model in the discovery set.



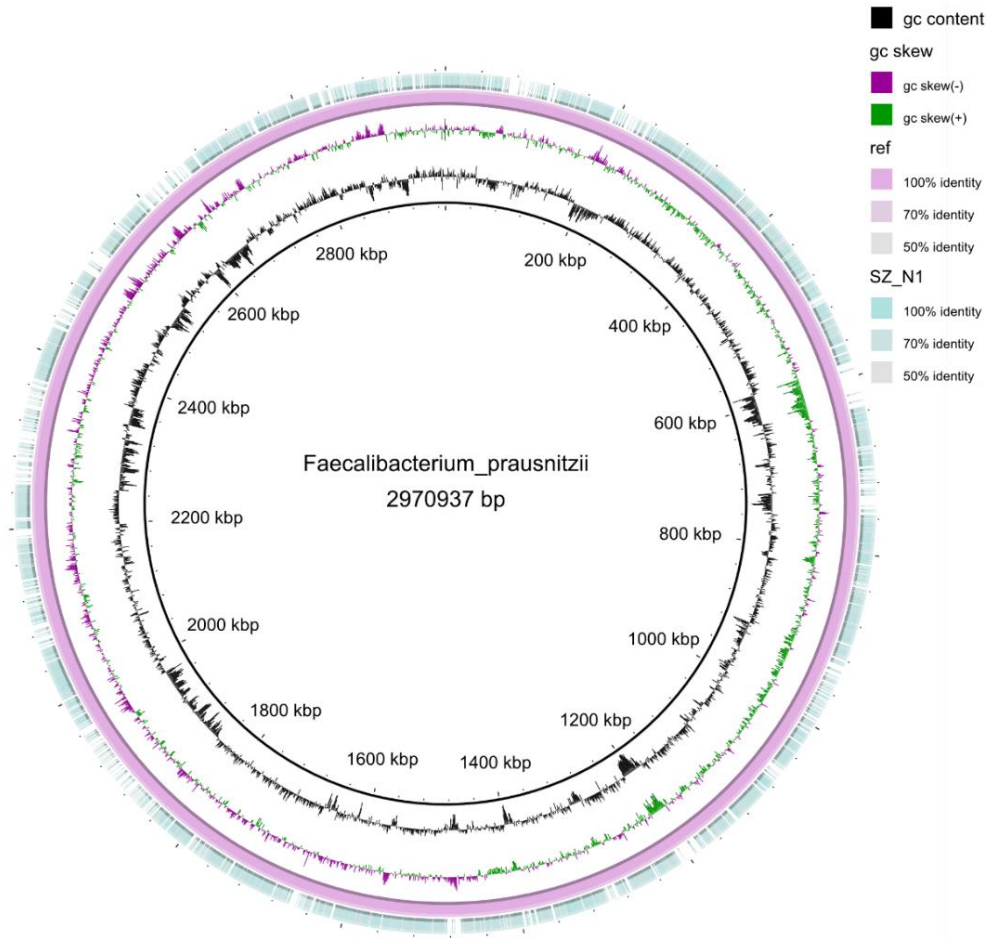
95 **Supplementary Figure 9. The Linear discriminant analysis effect size (LEfSe) analysis for the**  
 96 **discriminatory pathways between the NC and T1D group in the discovery set.**

97  
 98  
 99



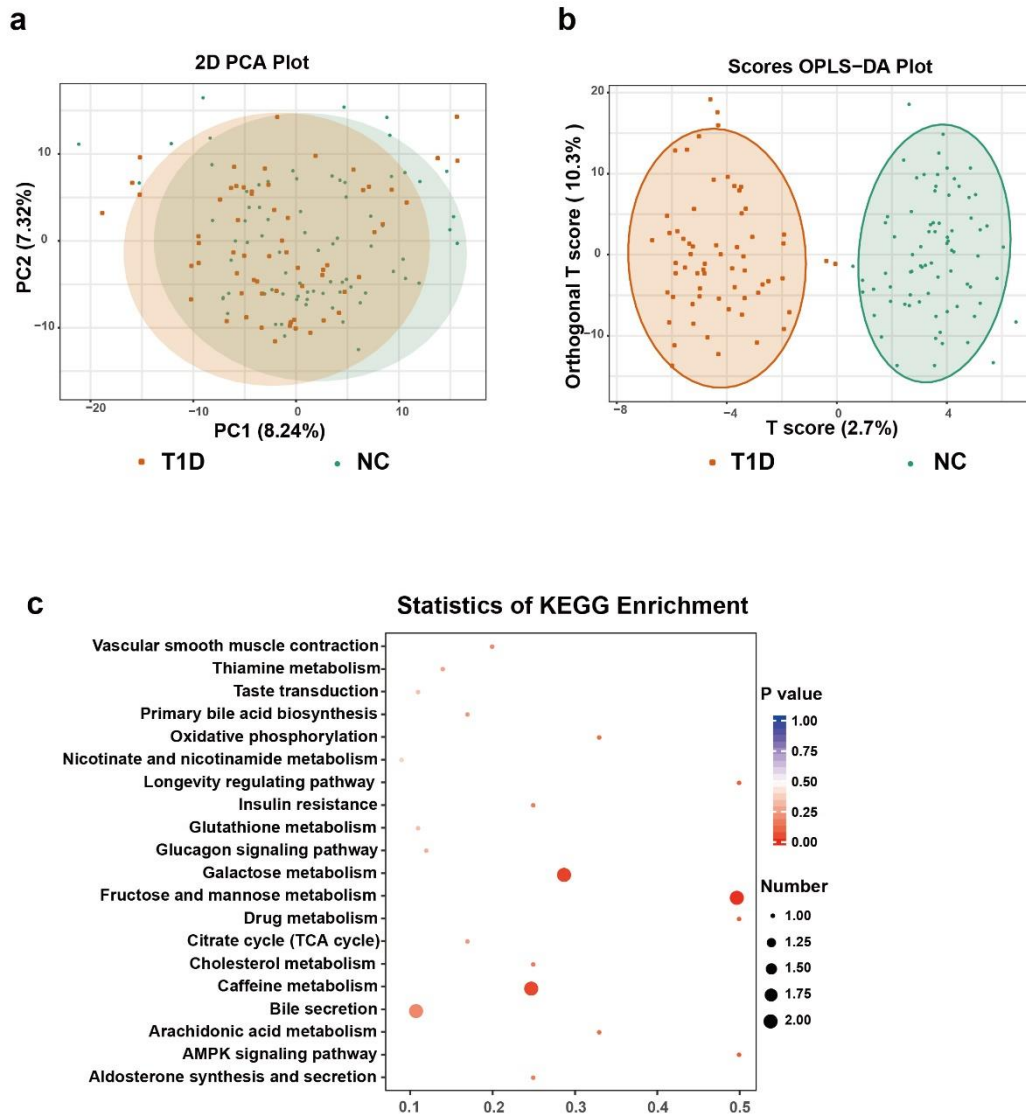
100 **Supplementary Figure 10. The shift in the relative abundance of CAZy gene families involved in**  
 101 **metabolizing different carbohydrate substrates in the discovery set.** *GH77*,  $p < 0.001$ ; *GH94*,  $p < 0.001$ ;  
 102 *GH16*,  $p = 0.005$ ; *GH53*,  $p = 0.026$ ; *GH43\_24*,  $p = 0.005$ ; *GH43\_3*,  $p = 0.012$ ; *GH5\_2*,  $p = 0.014$ ; *GH20*,  $p =$   
 103  $0.002$ ; *GH18*,  $p = 0.008$ ; *GH33*,  $p = 0.004$ ; *GH89*,  $p = 0.009$ ; *GH113*,  $p < 0.001$ ; *GH25*,  $p = 0.002$ ; *GH70*,  $p =$   
 104  $0.005$ ; *GH32*,  $p < 0.001$ ; *GH68*,  $p = 0.004$ ; *GH81*,  $p < 0.001$ ; *GH64*,  $p < 0.001$ ; *GH5\_9*,  $p < 0.001$ . Violin plots  
 105 show the median, quartiles, and min/max values. Two-sided Wilcoxon rank-sum test. \*  $p < 0.05$ , \*\*  $p < 0.01$ , \*\*\*  
 106  $p < 0.001$ .

107  
 108



109 **Supplementary Figure 11. High-quality draft genome of *Faecalibacterium prausnitzii*.** SZ\_N1 is the  
 110 representative sample with the highest relative abundance for *Faecalibacterium prausnitzii*.

111  
 112  
 113  
 114  
 115  
 116  
 117



118 **Supplementary Figure 12. Fecal metabolic profiles.** (a) PCA scores on samples between the NC and T1D  
 119 group. (b) The analyses of orthogonal partial least-squares discriminant analysis (OPLS-DA). (c) KEGG  
 120 pathway enrichment analysis between the NC and T1D group.

121

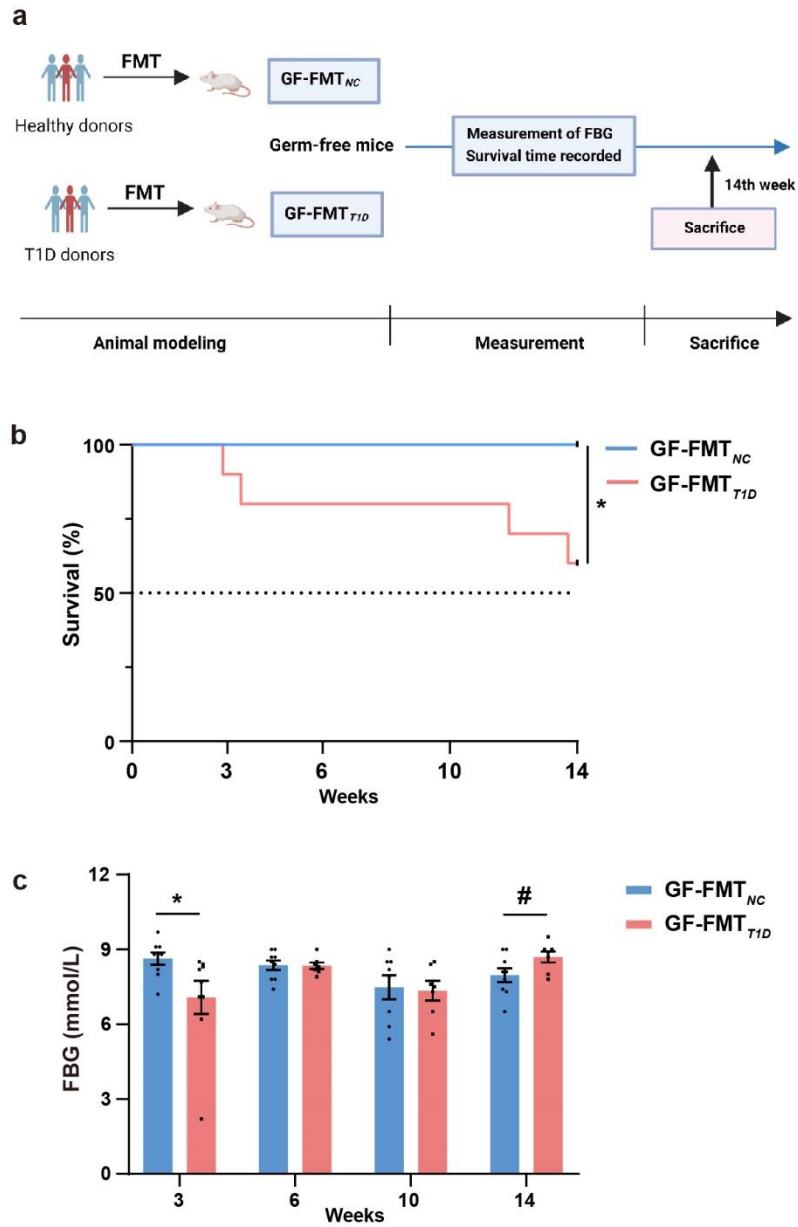
122

123

124

125

126



127 **Supplementary Figure 13. FMT with NC and T1D-associated gut microbiota in germ-free mice.** (a)  
 128 Schematic diagram of the study design. (b) Survival analysis of GF-FMT<sub>NC</sub> (n=9) and GF-FMT<sub>T1D</sub> (n=10) after  
 129 FMT ( $p = 0.038$ , Log-rank test). (c) Fasting blood glucose level after FMT. 3th week,  $p = 0.042$ ; 14th week,  $p =$   
 130  $0.091$ . Data represent the mean  $\pm$  SEM. Unpaired two-tailed t-test. \*  $p < 0.05$ , #  $0.05 < p < 0.1$ .

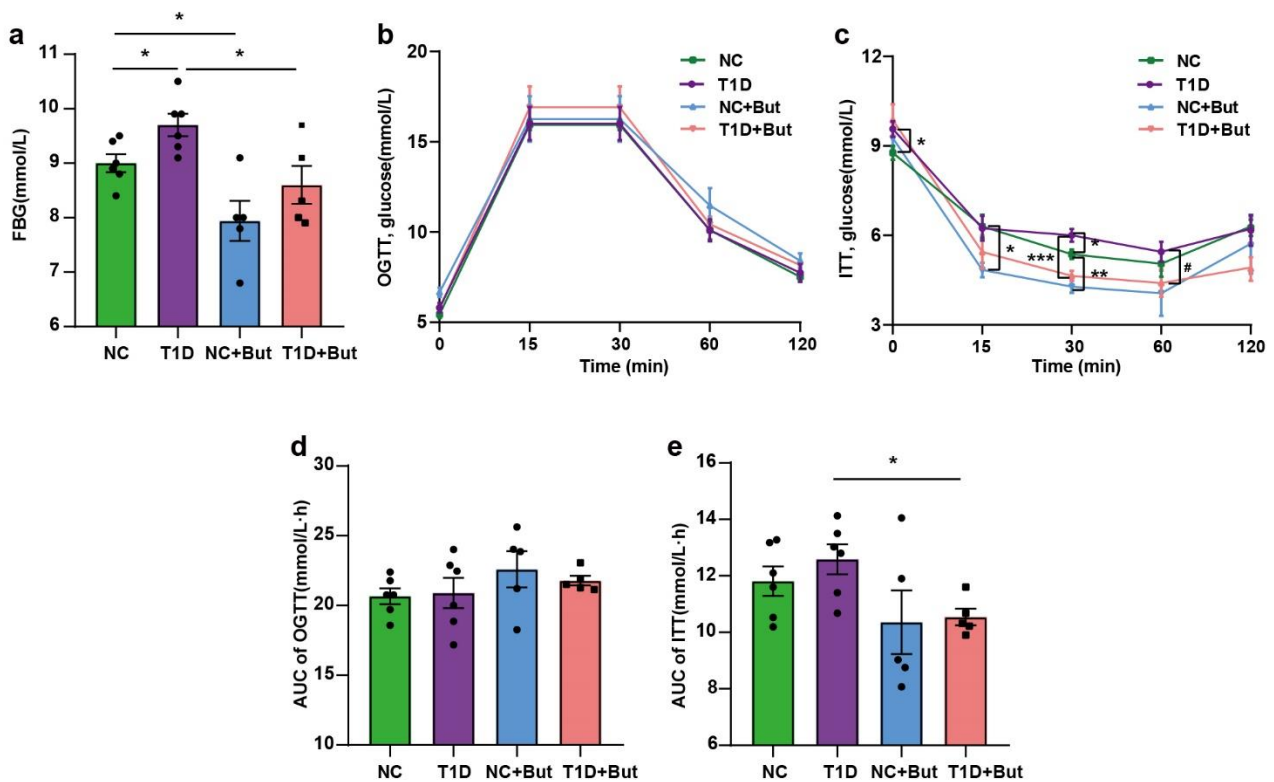
131

132

133

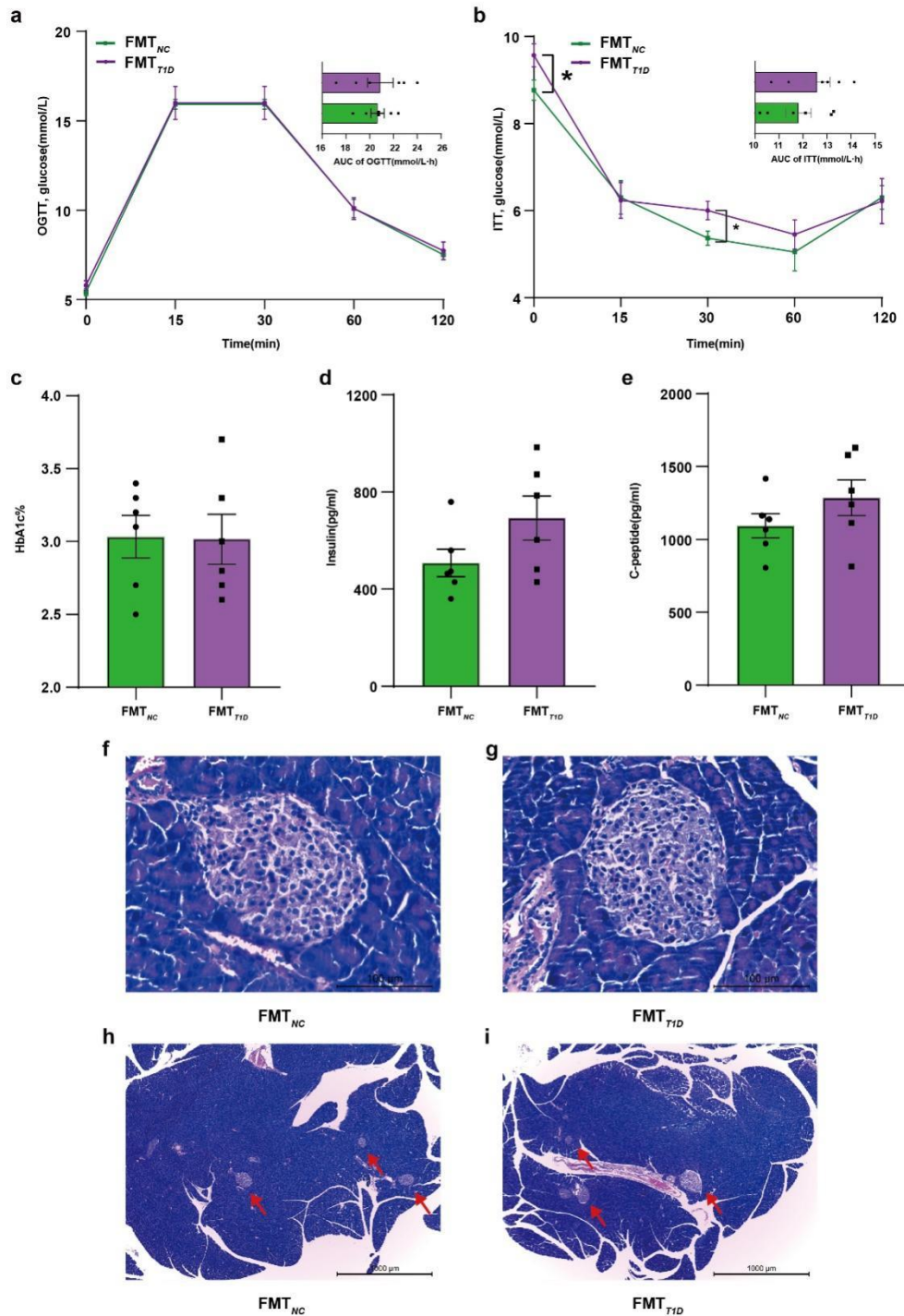
134

135



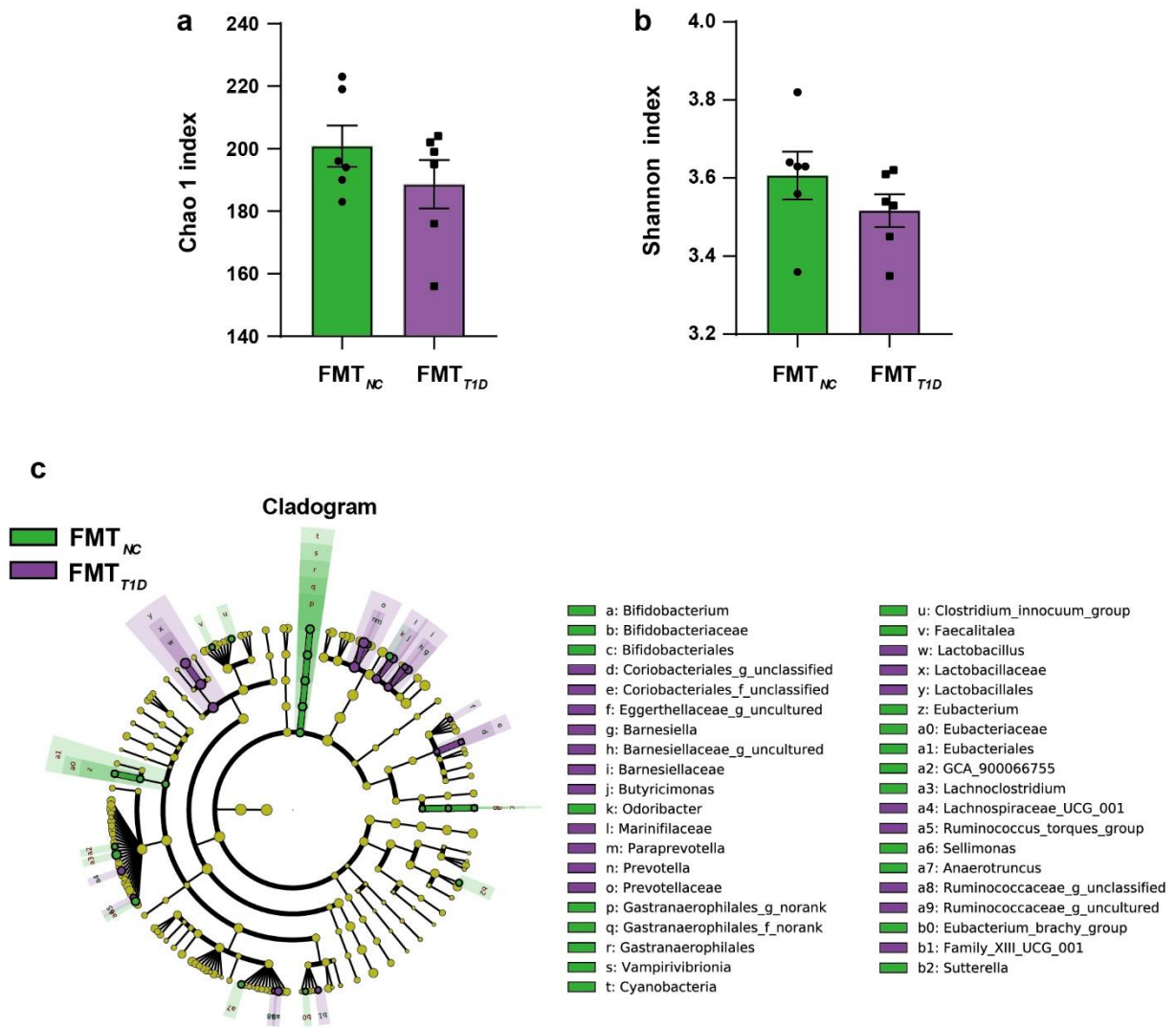
136 **Supplementary Figure 14. FMT with NC and T1D-associated gut microbiota in antibiotic-treated mice**  
 137 **with the supplement of butyrate.** (a) Fasting blood glucose levels in four groups (NC vs T1D,  $p = 0.025$ ; NC  
 138 vs NC+But,  $p = 0.020$ ; T1D vs T1D+But,  $p = 0.019$ ). (b, c) Glucose tolerance test (b) and Insulin tolerance test  
 139 (c) (0min, NC vs T1D,  $p = 0.046$ ; 15min, NC vs NC+But,  $p = 0.015$ ; 30min, NC vs T1D,  $p = 0.040$ ; NC vs NC+But,  
 140  $p = 0.003$ ; T1D vs T1D+But,  $p < 0.001$ ; 60min, T1D vs T1D+But,  $p = 0.094$ ). (d, e) The area under the curve  
 141 (AUC) in the OGTT (d) and ITT (e) (T1D vs T1D+But,  $p = 0.011$ ). NC, mice recipients FMT with NC gut microbiota  
 142 ( $n=6$ ); T1D, mice recipients FMT with T1D gut microbiota ( $n=6$ ); NC+But, NC mice recipients gavaged by  
 143 butyrate ( $n=5$ ); T1D+But, T1D mice recipients gavaged by butyrate ( $n=5$ ). Data represent the mean  $\pm$  SEM.  
 144 Unpaired two-tailed t-test. \*  $p < 0.05$ , \*\*  $p < 0.01$ , \*\*\*  $p < 0.001$ , #  $0.05 < p < 0.1$ .

145  
 146  
 147  
 148  
 149  
 150



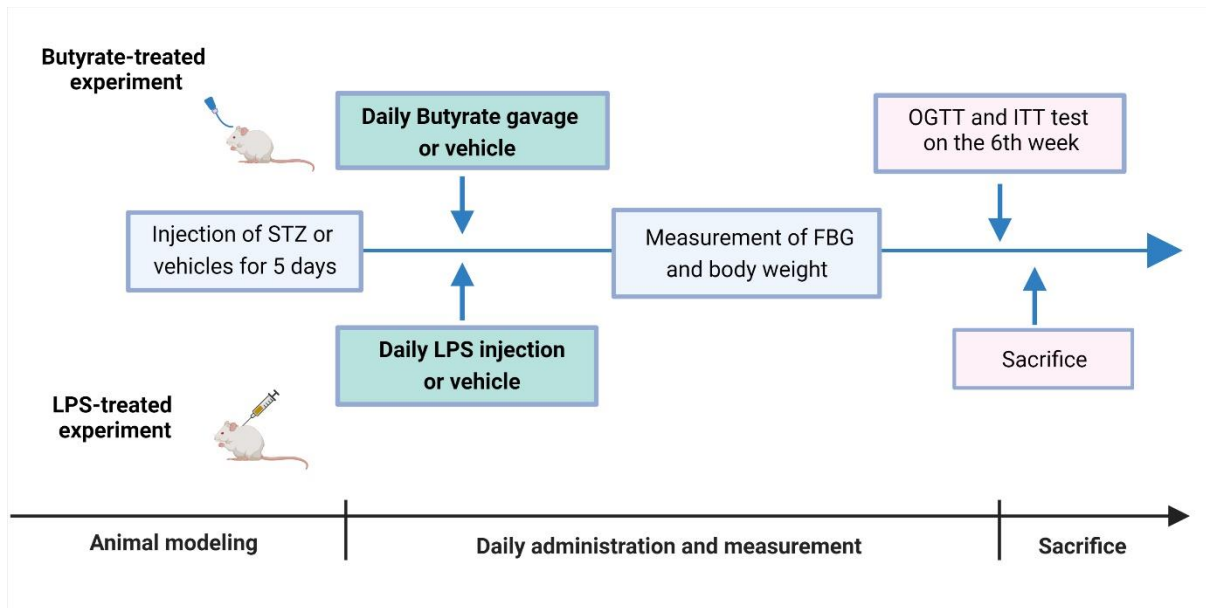
151 **Supplementary Figure 15. FMT with NC and T1D-associated gut microbiota in antibiotic-treated mice.**  
 152 (a, b) Glucose tolerance test and Insulin tolerance test (0min,  $p = 0.046$ ; 30min,  $p = 0.040$ ) with AUC. (c-e) The  
 153 level of HbA1c (c), insulin (d), and C-peptide (e) in the FMT<sub>NC</sub> (n=6) and FMT<sub>T1D</sub> (n=6) group. (f-i) HE staining  
 154 of the pancreas in two groups (400-fold and 40-fold magnification, respectively). Data represent the mean  $\pm$   
 155 SEM. Unpaired two-tailed t-test. \*  $p < 0.05$ .





156 **Supplementary Figure 16. The shift of gut microbiota based on 16S rRNA gene sequencing in the FMT<sub>NC</sub>**  
 157 **and FMT<sub>T1D</sub> groups.** (a, b) The microbial community richness (Chao 1 index; a) and diversity (Shannon index;  
 158 b). (c) Cladogram generated by LEfSe showing differences in bacterial taxa between the FMT<sub>NC</sub> and FMT<sub>T1D</sub>  
 159 groups. The color of discriminative taxa represents the taxa that are more abundant in the corresponding group  
 160 (FMT<sub>NC</sub> in green, FMT<sub>T1D</sub> in purple). n = 6 mice per group. Data represent the mean ± SEM. Unpaired two-tailed  
 161 t-test.

162  
 163  
 164



165 **Supplementary Figure 17. The animal experimental flowchart in butyrate-treated and LPS-treated**  
 166 **experiments.**

167

168

169

170

171

172

173

174

175

176

177

178

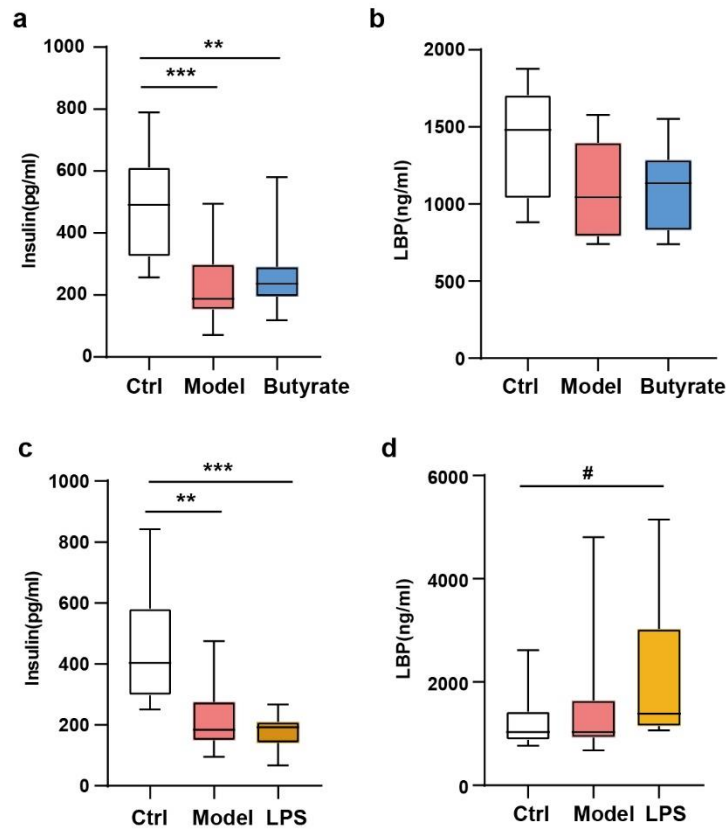
179

180

181

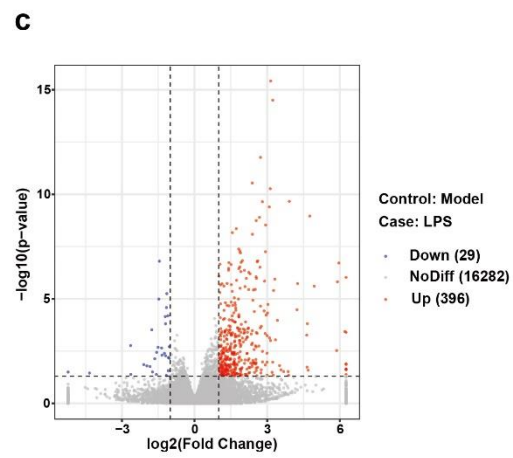
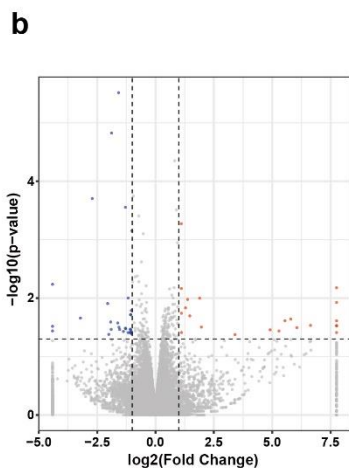
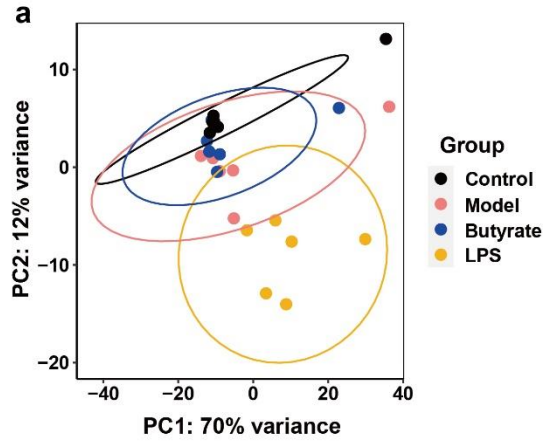
182

183



184 **Supplementary Figure 18. Serum insulin and LBP levels in butyrate-treated and LPS-treated**  
 185 **experiments.** (a, b) Serum insulin (a) (Ctrl vs Model,  $p < 0.001$ ; Ctrl vs Butyrate,  $p = 0.002$ ) and LBP (b) levels  
 186 in the butyrate-treated experiments. (c, d) Serum insulin (c) (Ctrl vs Model,  $p = 0.001$ ; Ctrl vs LPS,  $p < 0.001$ )  
 187 and LBP (d) levels (Ctrl vs LPS,  $p = 0.080$ ) in the LPS-treated experiments. Ctrl, control group; Model, STZ-  
 188 induced T1D group; Butyrate, STZ-induced T1D mice gavaged by butyrate; LPS, STZ-induced T1D mice  
 189 injected with LPS. In the butyrate-treated experiment, Ctrl:  $n = 10$ , Model:  $n = 11$ , Butyrate:  $n = 11$ ; in the LPS-  
 190 treated experiment, Ctrl:  $n = 10$ , Model:  $n = 12$ , LPS:  $n = 11$ . Box and whisker plots show median  $\pm$  quartiles (box),  
 191 min/max (whiskers). Unpaired two-sided t-test. \*\*  $p < 0.01$ , \*\*\*  $p < 0.001$ , #  $0.05 < p < 0.1$ .

192  
 193  
 194  
 195  
 196



197 **Supplementary Figure 19. RNA-sequencing analysis in butyrate-treated and LPS-treated experiments.**  
 198 (a) Principal component analysis (PCA) plot of RNA-seq datasets. (b, c) Volcano plot of differentially expressed  
 199 genes in butyrate-treated and LPS-treated experiments, respectively.